

Multicomponent Polyanions, 49

A Potentiometric and (^{31}P , ^{51}V) NMR Study of the Aqueous Molybdovanadophosphate SystemAnna Selling,^{*,[a]} Ingegärd Andersson,^[a] John H. Grate,^[b] and Lage Pettersson^[a]**Keywords:** Polyoxometalates / Phosphorus / Vanadium / Potentiometry / Formation constants

The equilibrium speciation of the quaternary system $\text{H}^+/\text{MoO}_4^{2-}/\text{HVO}_4^{2-}/\text{HPO}_4^{2-}$ in aqueous 0.600 M Na(Cl) at 25 °C and 90 °C was studied by pH potentiometry and ^{31}P (202.5 MHz) and ^{51}V (131.6 MHz) NMR spectrometry. The study focused on solutions containing the oxoanion components in the ratios $(\text{Mo} + \text{V})/\text{P} = 12:1$ and $\text{Mo}/\text{V} \geq 3.8$, in the pH range 0–5, wherein Keggin anions of the formula $[\text{H}_z\text{Mo}_{12-x}\text{V}_x\text{PO}_{40}]^{(3+x-z)-}$ with $x = 1-3$ are the predominant species. Formation constants ($\log \beta$) and $\text{p}K_a$ values for Keggin anions with $x = 1-3$ were determined from ^{31}P and ^{51}V

resonance chemical shift data, ^{31}P resonance intensity data, and pH potentiometric data with the multidata least squares calculation program LAKE. The $[\text{Mo}_{11}\text{VPO}_{40}]^{4-}$ anion does not protonate, $[\text{Mo}_{10}\text{V}_2\text{PO}_{40}]^{5-}$ anions can be monoprotonated, and $[\text{Mo}_9\text{V}_3\text{PO}_{40}]^{6-}$ anions can be triprotonated. The six most intense ^{31}P NMR resonances of $[\text{H}_z\text{Mo}_9\text{V}_3\text{PO}_{40}]^{(6-z)-}$ could be followed over the pH range studied. It was also possible to assign some ^{31}P resonances to a specific isomer of $[\text{Mo}_9\text{V}_3\text{PO}_{40}]^{6-}$.

Introduction

Speciation and structures in aqueous heteropoly- and isopolyoxometalate systems have been studied at Umeå University by potentiometric $[\text{H}^+]$ titrations and multinuclear NMR spectrometry. Data obtained by these methods were used in the least-squares calculation program LAKE,^[1] which can consider different types of data simultaneously; it thus proved possible to determine speciation and formation constants in complicated systems. These methods were applied in this study for characterising Keggin molybdovanadophosphate anions, $[\text{H}_z\text{Mo}_{12-x}\text{V}_x\text{PO}_{40}]^{(3+x-z)-}$, in the aqueous $\text{H}^+/\text{MoO}_4^{2-}/\text{HVO}_4^{2-}/\text{HPO}_4^{2-}$ system.^[2] Keggin molybdovanadophosphates are dioxygen-regenerable oxidants capable of mediating a variety of catalytic oxidation reactions,^[3] such as Wacker-like aqueous palladium-catalysed oxidations of olefins to carbonyls.^[4] Understanding the nature of the aqueous Keggin molybdovanadophosphates is essential to rational development of this chemical process and motivated the present study. We therefore studied acidic, aqueous molybdovanadophosphate solutions containing the oxoanion components in the ratio $(\text{Mo} + \text{V})/\text{P} = 12:1$, in which the Keggin molybdovanadophosphates, $[\text{H}_z\text{Mo}_{12-x}\text{V}_x\text{PO}_{40}]^{(3+x-z)-}$, are formed as the predominant species.

The α -Keggin structure, first reported by Keggin in 1933,^[5] is the structure encountered most frequently by far. Rotation of each M_3O_{13} group in turn by $\pi/3$ gives the β -, γ -, δ -, and ϵ -structures.^[6,7] These are increasingly disfavoured, in this order, by increasing internal electrostatic repulsions of the M atoms. Some β -structures and, recently, one γ -structure^[8] have been reported for XM_2^{VI} species, but we are unaware of any δ - and ϵ -structures. β -Structures become more likely when the internal electrostatic repulsions are decreased, either by the substitution of M^{VI} by lower-valence M atoms or by the reduction of M^{VI} atoms.

In the parent α -Keggin $[\text{Mo}_{12}\text{PO}_{40}]^{3-}$ structure, which has T_d symmetry, all Mo sites are equivalent by symmetry, so that one isomorphous substitution of V for Mo results in a single α - $[\text{Mo}_{11}\text{VPO}_{40}]^{4-}$ structure. By isomorphous substitution of two, three, or four V for Mo, 5, 13, or 27 positional α -Keggin isomers and an increasing number of β -isomers can be formed.^[7] Consequently, the present study was restricted to solutions containing Keggin molybdovanadophosphates with $x \leq 3$ to somewhat simplify this complicated system.

The binary $\text{H}^+/\text{HVO}_4^{2-}$,^[9-11] $\text{H}^+/\text{MoO}_4^{2-}$,^[12] and $\text{H}^+/\text{HPO}_4^{2-}$ ^[13] and the ternary $\text{H}^+/\text{HVO}_4^{2-}/\text{HPO}_4^{2-}$,^[13] $\text{H}^+/\text{MoO}_4^{2-}/\text{HPO}_4^{2-}$,^[14,15] and $\text{H}^+/\text{MoO}_4^{2-}/\text{HVO}_4^{2-}$ ^[16,17] subsystems in 0.6 M Na(Cl) at 25 °C have all been previously characterised and are used in the present study of the quaternary system. The present study was extended to a higher temperature, 90 °C, to assess the effect of temperature on speciation. Many applications of Keggin molybdovanadophosphates in oxidation reactions^[4] are performed at such elevated temperatures.

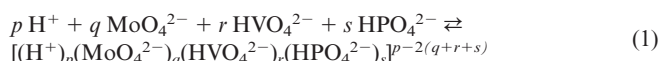
^[a] Department of Inorganic Chemistry, Umeå University
SE-90187 Umeå Sweden
Fax: (internat.) +46-90/786 9195
E-mail: anna.selling@chem.umu.se

^[b] Catalytica Inc.,
430 Ferguson Drive, Mountain View, California 94043, U.S.A.

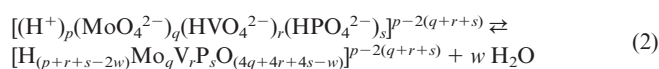
Our ^{31}P - and ^{51}V -NMR characterisation of the isomeric Keggin decamolybdovanadophosphate ions, $x = 2$, at 25 °C and 90 °C, and their individual $\text{p}K_{\text{a}}$ values, has already been reported.^[18] Many of the conclusions presented herein for the Keggin nonamolybdotriphosphates, $x = 3$, rely substantially, by analogy, on the findings presented in that report. Some preliminary results from the present study were presented earlier at an international workshop.^[19]

Notations and Designations

The polyanion formation constants are reported with H^+ , MoO_4^{2-} , HVO_4^{2-} , and HPO_4^{2-} as the components, and equilibria are written according to Equation (1).



The resulting polyanions will, for brevity, sometimes be denoted by their (p,q,r,s) integers and formation constants are reported as $\beta_{p,q,r,s}$. The potentiometric $[\text{H}^+]$ -titration data establish only the composition, that is, (p,q,r,s) , of the various polyanions. Their actual ionic formulae are related to their (p,q,r,s) values by loss of water, Equation (2).



Complementary structural information, such as NMR and X-ray data, is required to establish the formulae. Compositions given in brackets, as in $[\text{HMo}_9\text{V}_3\text{PO}_{40}]^{5-}$, designate the ionic formulae of discrete Keggin ions. To designate Keggin structures without regard to protonation state and charge, the abbreviated form $\text{Mo}_9\text{V}_3\text{P}$ is sometimes used.

Compositions given in braces, as in $\{\text{Na}_5\text{HMo}_9\text{V}_3\text{PO}_{40}\}$, designate the macroscopic elemental compositions of certain solutions and solids of Keggin salts. This designation rigorously specifies the known mole ratios of Na, Mo, V, and P present. In the solids and in the majority of solutions,

Mo, V and P are present in exactly the Keggin proportions, $(\text{Mo} + \text{V}) = 12 \text{ P}$, and are predominantly incorporated into Keggin anions. The macroscopic composition in braces therefore corresponds, essentially, to the average Keggin anion formula and the counteranions present to balance its average anionic charge. These average formulae in braces can have nonintegral ratios of the elements.

To designate the positional isomers of α and β Keggin species, the recommended IUPAC numbering schemes are used.^[20] Like Pope^[21] and most other authors, however, we indicate the vanadium positions in Keggin molybdovanadophosphates by the lowest possible numbers (1,*a,b* for α - $[\text{Mo}_9\text{V}_3\text{PO}_{40}]^{6-}$ isomers), not by the highest possible numbers (12,*c,d*) as in the recommended IUPAC schemes. In this paper, all references to dissymmetric positional isomers refer to both enantiomers together.

The acidity measurements are on the concentration scale, where $\text{pH} = -\log [\text{H}^+]$, not on the activity scale, where $\text{pH} = -\log \{\text{H}^+\}$. We will, for simplicity, use pH instead of $-\log [\text{H}^+]$. For brevity, the total concentrations of molybdenum, vanadium, and phosphorus are often denoted by Mo, V, and P.

Results and Discussion

Equilibrium Analysis

Since the present study focused on solutions containing the oxoanion components in the ratio $(\text{Mo} + \text{V})/\text{P} = 12:1$, in the pH range 0–5, the predominant oxoanion species present were the Keggin anions, $[\text{H}_z\text{Mo}_{12-x}\text{V}_x\text{PO}_{40}]^{(3+x-z)-}$. Figure 1 maps the solutions, in (Mo/V) vs. pH space, for which data were collected.

The equilibrium calculations were simplified by the use of data only from solutions with $\text{Mo}/\text{V} \geq 3.8$, and in these solutions only $[\text{H}_z\text{Mo}_{12-x}\text{V}_x\text{PO}_{40}]^{(3+x-z)-}$ species with $x =$

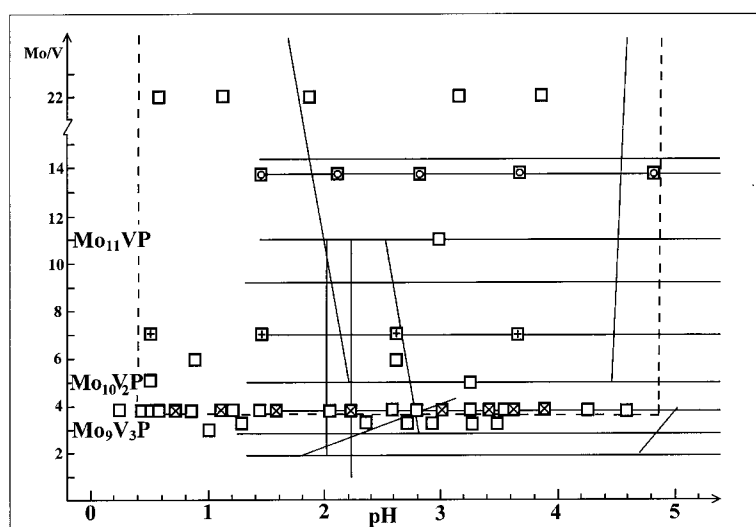










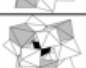




Figure 1. Mo/V ratios and pH values of Keggin molybdovanadophosphate solutions for which experimental data were collected by EMF titrations (continuous lines) from ^{31}P - and ^{51}V -NMR spectroscopy (\square). Note the break in the Mo/V scale. The data used in the equilibrium calculations is from solutions within the dashed lines. NMR data from the points marked with \circ , $+$, and \times are included in the distribution diagrams of Figures 3, 4, and 5, respectively

Table 1. Polyhedral structures of the thirteen positional isomers of α -[Mo₉V₃PO₄₀]⁶⁻ with their designation, symmetry point group, statistically predicted abundance in these α -isomers, and ³¹P NMR resonance assignment (Figure 8). The VO₆ octahedra are shaded. Statistically predicted abundance 1 is for the α -isomers only. Statistically predicted abundance 2 is found for both the α - and β -isomers when approx. 17% of phosphorus is bound in β -isomers (see text)

Polyhedral Structure	Designation (enantiomer)	Symmetry	Statistical Abundance 1	Assignment ³¹ P	Statistical Abundance 2	Integral
	α -1,4,9	C_{3v}	1.82 %	Resonance 1	1.5 %	0.8 %
	α -1,2,3	C_{3v}	1.82 %	Resonance 2	1.5 %	2.7 %
	α -1,2,4 (α -1,3,9)	C_I	10.9 %	Resonance 3	9.1 %	28 %
	α -1,2,6 (α -1,3,7)	C_I	10.9 %		9.1 %	
	α -1,4,8 (α -1,5,9)	C_I	10.9 %		9.1 %	
	α -1,4,6	C_S	5.46 %	Resonance 4	4.5 %	5.2 %
	α -1,2,8 (α -1,3,5)	C_I	10.9 %	Resonance 5	9.1 %	20 %
	α -1,4,7 (α -1,6,9)	C_I	10.9 %		9.1 %	
	α -1,2,10	C_S	5.46 %		4.5 %	
	α -1,2,11 (α -1,3,11)	C_I	10.9 %		9.1 %	
	α -1,5,8	C_S	5.46 %		4.5 %	
	α -1,5,7 (α -1,6,8)	C_I	10.9 %		9.1 %	
	α -1,6,12 (α -1,7,10)	C_3	3.61 %		3.0 %	

1–3 are present. Solutions with Mo/V < 3.8 contain [H₂Mo₈V₄PO₄₀]⁽⁷⁻²⁾⁻ species and, at lower Mo/V, even higher V-content species. ³¹P- and ⁵¹V-NMR data from solutions with Mo/V < 3.8 were collected to help in assigning resonances and obtaining accurate relative abundances (by resonance integration) for the isomeric Mo₉V₃P species.

α -Keggin compositions with $x \geq 2$ can exist as positional isomers. Table 1 shows the polyhedral structures, symmetries, and statistically predicted relative abundances for the α -isomers of Mo₉V₃P. We were able to track the pH dependence of the ³¹P resonances of the more abundant, but not all, Mo₉V₃P isomers at 25 °C. Figure 2 shows the ³¹P chemical shifts of six Mo₉V₃P resonances plotted against pH over the range 0–6, along with the ³¹P chemical shift vs. pH dependence for [Mo₁₁VPO₄₀]⁴⁻ and the Mo₁₀V₂P isomers determined previously.^[18]

Equilibrium calculations were directed at identifying the Keggin compositions, [H₂Mo_{12-x}V_xPO₄₀]^{(3+x-2)-}, present and for determining their formation constants, for $x = 1$ –3. The equilibrium analysis of this system is complicated by two factors. First, the Keggin species exist in solution as

equilibrium distributions over compositions of varying x , centred on the solution bulk composition. Consequently, it is not possible to EMF titrate species that have one x composition in the near absence of species of higher and lower x compositions. (The exception is [Mo₁₁VPO₄₀]⁴⁻ ($x = 1$), which is present only as the single α -isomer, which remains unprotonated up to pH < 0, and does not significantly disproportionate at equilibrium into $x = 0$ and $x = 2$ species.^[18]) Second, compositions with $x \geq 2$ exist as equilibrium mixtures of isomers, each with its own pK_a, which cannot be individually EMF titrated. Consequently, EMF titration data for solutions containing Mo₁₀V₂P and Mo₉V₃P compositions manifest simultaneous titrations of numerous species.

The data from EMF titrations at different Mo/V ratios allow the calculations to distinguish the titration of the abundance-weighted average $x = 2$ species from the titration of the abundance-weighted average $x = 3$ species. Only the NMR chemical shifts vs. pH data (equivalent to spectrometric titrations) allow the titration curves, and thus the pK_a values and formation constants, of individual isomeric

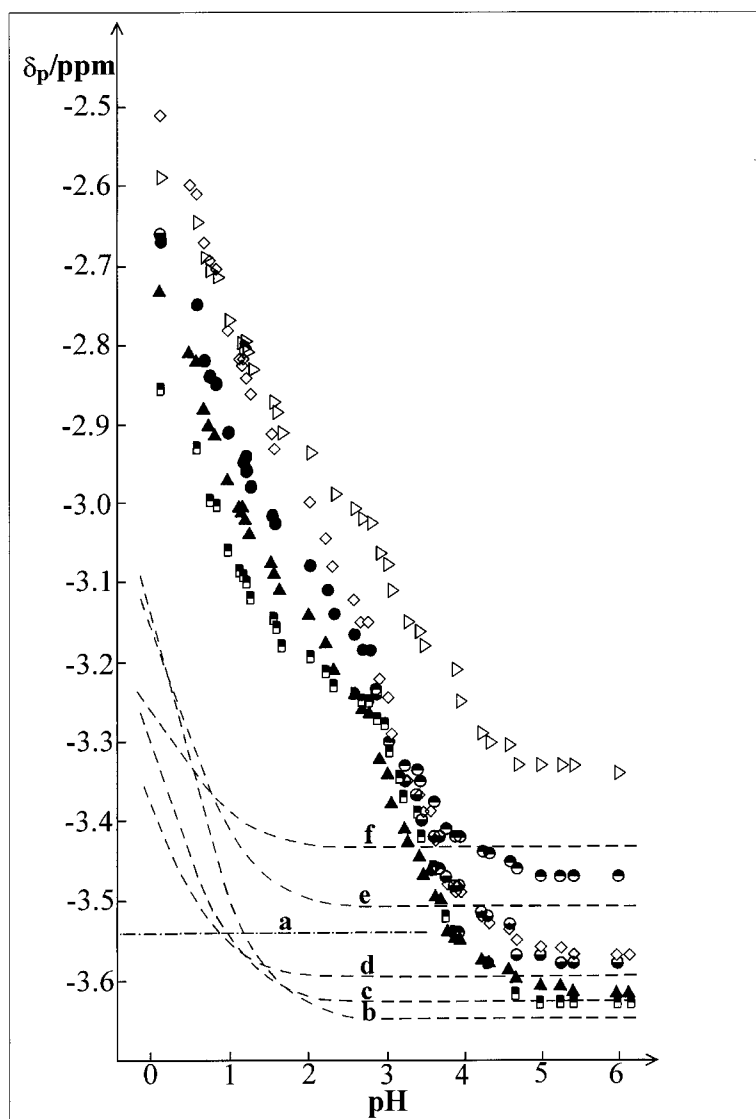


Figure 2. ^{31}P chemical shifts, at 25 °C, of the most intense Keggin $\text{Mo}_9\text{V}_3\text{P}$ isomers, plotted as a function of pH. The dashed dotted line (a) shows the chemical shift of $[\text{Mo}_{11}\text{VPO}_{40}]^{4-}$ and the dashed curves (b–f) show the chemical shifts of the $\text{Mo}_{10}\text{V}_2\text{P}$ isomers: b: α -1,4; c: α -1,2 + α -1,5; d: α -1,6 + α -1,11; e, f: β -4,10 and β -4,11^[18]

species to be distinguished. For the $\text{Mo}_{10}\text{V}_2\text{P}$ composition, it proved possible to resolve and track the ^{31}P - and ^{51}V -NMR resonances of the different isomers against pH sufficiently to assign the resonances to isomeric structures, to determine the $\text{p}K_{\text{a}}$ values of the monoprotonated anions, and to evaluate their relative abundances.^[18] Those data have been used to calculate the individual formation constants of $[\text{H}_z\text{Mo}_{10}\text{V}_2\text{PO}_{40}]^{(5-z)-}$ species where $z = 0, 1$, as described below. As mentioned earlier, it was not possible to resolve and track the resonances of all the significant $\text{Mo}_9\text{V}_3\text{P}$ isomers over pH, either by ^{31}P - or ^{51}V -NMR, and only “average” $\text{p}K_{\text{a}}$ values and formation constants for these isomers could be determined.

To establish the formation constants for the $[\text{H}_z\text{Mo}_{12-x}\text{V}_x\text{PO}_{40}]^{(3+x-z)-}$ compositions, the EMF potentiometric and NMR data were extensively evaluated with

the LAKE multimethod least-square program, as described below. The “best” model obtained is reported in Table 2.

The determination of the formation constants began with the evaluation of the combined EMF and NMR integral data for solutions with the oxoanion component ratios $(\text{Mo}+\text{V})/\text{P} \geq 11.8$. At Mo/V ratios above or at 13.75, α - $[\text{Mo}_{11}\text{VPO}_{40}]^{4-}$ is strongly favoured over compositions with higher vanadium content, and is the only molybdovanadophosphate species present at $\text{pH} < 2$. Because this composition contains so much more P and Mo than in the Mo_{11}VP Keggin composition, some molybdophosphate species are also present in these solutions. Since the formation constants of the species in the molybdophosphate system were previously determined in the same ionic medium,^[15] the formation constant of α - $[\text{Mo}_{11}\text{VPO}_{40}]^{4-}$ could be determined accurately.

Table 2. The formation constants of $[\text{Mo}_{11}\text{VPO}_{40}]^{4-}$, $[\text{H}_z\text{Mo}_{10}\text{V}_2\text{PO}_{40}]^{(5-z)-}$ ($z = 0, 1$), and $[\text{H}_z\text{Mo}_9\text{V}_3\text{PO}_{40}]^{(6-z)-}$ ($z = 0, 1, 2, 3$), based on EMF data, NMR integral data for the molybdovanadophosphate species and the ^{31}P chemical shift data for the $\text{Mo}_{10}\text{V}_2\text{P}$ species and the most intense $\text{Mo}_9\text{V}_3\text{P}$ resonance. The formation constants reported for the $\text{Mo}_{10}\text{V}_2\text{P}$ and $\text{Mo}_9\text{V}_3\text{P}$ compositions are each the abundance-weighted average formation constants over all the isomeric species with that composition

NMR symbol	(<i>p, q, r, s</i>) notation	Formula	$\log \beta \pm (3\sigma)$	$\text{p}K_a$
Δ	22,11,1,1	$\text{Mo}_{11}\text{VPO}_{40}^{4-}$	141.5 (2)	
○	21,10,2,1	$\text{Mo}_{10}\text{V}_2\text{PO}_{40}^{5-}$	146.9 (3)	
	22,10,2,1	$\text{HMo}_{10}\text{V}_2\text{PO}_{40}^{4-}$	147.2 (3)	0.3
◇	20,9,3,1	$\text{Mo}_9\text{V}_3\text{PO}_{40}^{6-}$	147.1 (3)	
	21,9,3,1	$\text{HMo}_9\text{V}_3\text{PO}_{40}^{5-}$	150.2 (3)	3.1
	22,9,3,1	$\text{H}_2\text{Mo}_9\text{V}_3\text{PO}_{40}^{4-}$	151.7 (3)	1.5
	23,9,3,1	$\text{H}_3\text{Mo}_9\text{V}_3\text{PO}_{40}^{3-}$	152.2 (3)	0.5

By next expanding the evaluation to include data from solutions in which $\text{Mo}_{10}\text{V}_2\text{P}$ species are also present, but in which $\text{Mo}_9\text{V}_3\text{P}$ species are still absent, the formation constants for the $\text{Mo}_{10}\text{V}_2\text{P}$ compositions were determined. In addition to the combined EMF and NMR integral data for such solutions, this evaluation also included the chemical shift vs. pH data for the ^{51}V resonance of the α -1,2- $[\text{H}_z\text{Mo}_{10}\text{V}_2\text{PO}_{40}]^{(5-z)-}$ ($z = 0, 1$) isomer. This isomer was chosen as a surrogate for the average $\text{Mo}_{10}\text{V}_2\text{P}$ composition, as its $\text{p}K_a$ (0.26) is midway between the most extreme $\text{p}K_a$ values of the $\text{Mo}_{10}\text{V}_2\text{P}$ isomers (0.04 for α -1,6 + α -1,11 and 0.48 for α -1,4).^[18] The formation constants so determined for $[\text{Mo}_{10}\text{V}_2\text{PO}_{40}]^{5-}$ and $[\text{HMo}_{10}\text{V}_2\text{PO}_{40}]^{4-}$ are essentially the abundance-weighted average formation constants for the manifold of $\text{Mo}_{10}\text{V}_2\text{P}$ isomers. (They are strictly this average except to the extent that the surrogate $\text{p}K_a$ differs from the actual average $\text{p}K_a$.)

The solutions whose data were used to determine formation constants for the $\text{Mo}_{10}\text{V}_2\text{P}$ compositions included solutions with the oxoanion component ratios $(\text{Mo} + \text{V})/\text{P} \geq 11.8$, as above, but at $\text{pH} > 2$. Above $\text{pH} = 2$, $[\text{Mo}_{11}\text{VPO}_{40}]^{4-}$ is partly ($\text{pH} = 2$ –4) or completely ($\text{pH} > 4$) disproportionated to molybdophosphate species and $\text{Mo}_{10}\text{V}_2\text{P}$ species at equilibrium. Figure 3 shows a phosphorus distribution diagram for solutions of this composition over the entire pH range of this study, 0–5. Experimental points from the ^{31}P -NMR integral data are included in Figure 3, showing that the fit of experimental data to the calculated formation constants is good.

Also among the solutions containing $\text{Mo}_{10}\text{V}_2\text{P}$ species, but not $\text{Mo}_9\text{V}_3\text{P}$ species, that were used to determine the $\text{Mo}_{10}\text{V}_2\text{P}$ formation constants, were solutions with the oxoanion components in the Keggin ratio $(\text{Mo} + \text{V})/\text{P} = 12.0$ and with the Mo/V ratio decreased to above or equal to 7 (average composition $\text{Mo}_{10.5}\text{V}_{1.5}\text{P}$). Figure 4 shows a calculated phosphorus distribution diagram as a function of pH and experimental ^{31}P NMR integral data points for solutions of this composition, with $\text{Mo}/\text{V} = 7$.

After the evaluation was expanded to include EMF, NMR integral, and shift data from solutions with the Mo/V ratio decreased to above or at 3.8 (average composition

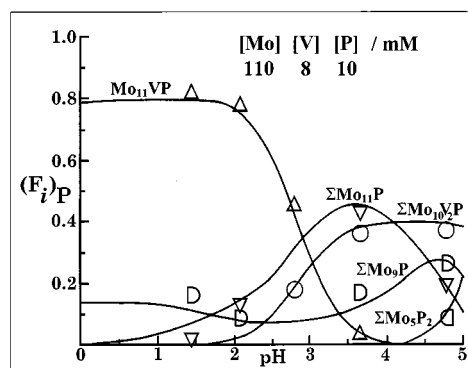


Figure 3. Distribution diagram of phosphorus-containing species as a function of pH in a solution with the oxoanion components in the ratio $(\text{Mo} + \text{V})/\text{P} = (11 + 0.8):1 = 11.8$ and 10 mM P. $(F_i)_P$ is the fraction of the total phosphorus. At this ratio, some well-known molybdophosphate species, Mo_{11}P , Mo_9P , and Mo_5P_2 , are present. The symbols represent experimental ^{31}P -NMR integral data

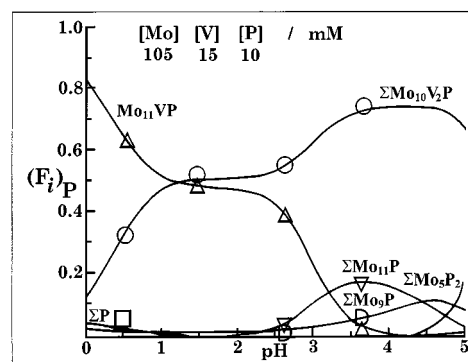


Figure 4. Distribution diagram of phosphorus-containing species as a function of pH in a solution with oxoanion components in the ratio $(\text{Mo} + \text{V})/\text{P} = (10.5 + 1.5):1$ and 10 mM P. The symbols represent experimental ^{31}P -NMR integral data

$\text{Mo}_9\text{V}_3\text{P}$), the formation constants for the $\text{Mo}_9\text{V}_3\text{P}$ compositions were determined. The final calculation is a simultaneous variation of all constants in which all kinds of data with $\text{Mo}/\text{V} \geq 3.8$ are used, and the result is shown in Table 2. Only the ^{31}P chemical shift data vs. pH for the highest intensity $\text{Mo}_9\text{V}_3\text{P}$ resonance (▲ in Figure 2) were included. A model with four $[\text{H}_z\text{Mo}_9\text{V}_3\text{PO}_{40}]^{(6-z)-}$ compositions ($z = 0, 1, 2, 3$) gave the best explanation of included data. (For the manifold of $\text{Mo}_9\text{V}_3\text{P}$ isomers, the pH dependence of the chemical shift of the most intense ^{31}P resonance was taken as a surrogate for the abundance-weighted average pH dependence.)

The $\text{p}K_a$ values for the highest intensity $\text{Mo}_9\text{V}_3\text{P}$ ^{31}P -NMR resonance (▲ in Figure 2) were also determined in a LAKE calculation in which only the chemical shift vs. pH data were used. These $\text{p}K_a$ values ($\text{p}K_{a3} = 3.18$, $\text{p}K_{a2} = 1.66$, $\text{p}K_{a1} = 0.56$) agree well with the three $\text{p}K_a$ values determined by equilibrium in Table 2 ($\text{p}K_{a3} = 3.1$, $\text{p}K_{a2} = 1.5$, $\text{p}K_{a1} = 0.5$).

Figure 5 shows a distribution diagram of phosphorus, as a function of pH, at a $\text{Mo}/\text{V} = 3.8$ ratio, based on the results showed in Table 2. In this figure, each of the protonation states is plotted individually with dotted lines and the solid lines show the sums of “homonuclear” species.

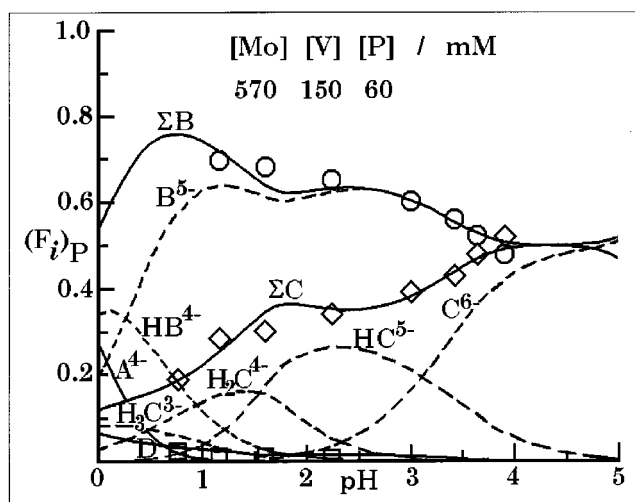


Figure 5. Distribution diagram of phosphorus-containing species as a function of pH in a solution with the oxoanion components in the ratio (Mo + V)/P = (9.5 + 2.5):1 and 60 mM P. Each of the protonation states is plotted individually with dotted lines and the solid lines show the sums of “homonuclear” species. $\mathbf{A}^{4-} = [\text{Mo}_{11}\text{VPO}_{40}]^{4-}$; $\mathbf{B}^{5-} = [\text{Mo}_{10}\text{V}_2\text{PO}_{40}]^{5-}$; $\mathbf{HB}^{4-} = [\text{HMo}_{10}\text{V}_2\text{PO}_{40}]^{4-}$; $\mathbf{\Sigma B} = \mathbf{B}^{5-} + \mathbf{HB}^{4-}$; $\mathbf{C}^{6-} = [\text{Mo}_9\text{V}_3\text{PO}_{40}]^{6-}$; $\mathbf{HC}^{5-} = [\text{HMo}_9\text{V}_3\text{PO}_{40}]^{5-}$; $\mathbf{H}_2\text{C}^{4-} = [\text{H}_2\text{Mo}_9\text{V}_3\text{PO}_{40}]^{4-}$; $\mathbf{H}_3\text{C}^{3-} = [\text{H}_3\text{Mo}_9\text{V}_3\text{PO}_{40}]^{3-}$; $\mathbf{\Sigma C} = \mathbf{C}^{6-} + \mathbf{HC}^{5-} + \mathbf{H}_2\text{C}^{4-} + \mathbf{H}_3\text{C}^{3-}$; $\mathbf{D} = \text{H}_3\text{PO}_4$. The symbols represent experimental ^{31}P -NMR integral data

NMR integral data have an error of about 5–10%, which can explain the disparity between the model and the experimental data in the figure. In this solution $\text{Mo}_{10}\text{V}_2\text{P}$ species contain 40–50% of the total amount of vanadium and 60–70% of phosphorus over almost the entire pH range.

The relative abundances of the $[\text{Mo}_{10}\text{V}_2\text{PO}_{40}]^{5-}$ isomers, determined previously,^[18] and the abundance-weighted average formation constant determined in this study (Table 2) were used for calculating the formation constants of the individual $[\text{Mo}_{10}\text{V}_2\text{PO}_{40}]^{5-}$ isomers; these are reported in Table 3. The $\text{p}K_{\text{a}}$ values determined for the conjugate, monoprotonated $[\text{HMo}_{10}\text{V}_2\text{PO}_{40}]^{4-}$ isomers^[18] were used

Table 3. Individual formation constants for the $[\text{H}_2\text{Mo}_{10}\text{V}_2\text{PO}_{40}]^{(5-z)-}$ ($z = 0, 1$) isomers, calculated from the abundance-weighted average formation constants for the composition, their relative abundances among themselves (NMR integral data), and their $\text{p}K_{\text{a}}$ values; the latter data is from ref.^[18]

(p,q,r,s) notation	Formula	IUPAC notation	$\log \beta$	pK_a
21,10,2,1	$\text{Mo}_{10}\text{V}_2\text{PO}_{40}^{5-}$		146.93	
		α -1,4	145.97	
		α -1,2	146.25	
		α -1,5	146.25	
		α -1,6+ α -1,11	146.53	
		β	145.53	
		β	145.41	
22,10,2,1	$\text{HMo}_{10}\text{V}_2\text{PO}_{40}^{4-}$		147.19	0.26
		α -1,4	146.45	0.48
		α -1,2	146.51	0.26
		α -1,5	146.51	0.26
		α -1,6+ α -1,11	146.57	0.04
		β	145.88	0.35
		β	145.74	0.33

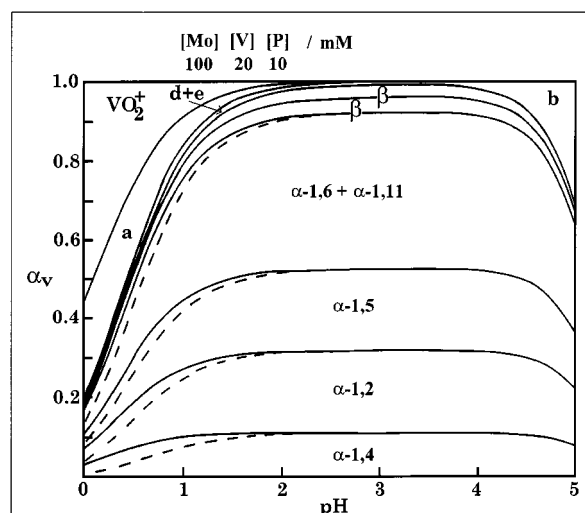


Figure 6. Diagram showing the cumulative distribution of vanadium-containing species, α_v , as a function of pH in solutions; the oxoanion components appear in the ratio (Mo + V)/P = (10 + 2):1, at P = 10 mm. The area between a solid curve and the dashed curve below it represent the protonated species, $[\text{HMo}_{10}\text{V}_2\text{PO}_{40}]^{4-}$. **a:** $[\text{Mo}_{11}\text{VPO}_{40}]^{4-}$; **b:** $[\text{Mo}_9\text{V}_3\text{PO}_{40}]^{6-}$; **d:** $[\text{H}_2\text{Mo}_9\text{V}_3\text{PO}_{40}]^{4-}$; **e:** $[\text{H}_3\text{Mo}_9\text{V}_3\text{PO}_{40}]^{3-}$

for the determination of their formation constants (Table 3).

Figure 6 shows a calculated vanadium distribution diagram, distinguishing between the individual $\text{Mo}_{10}\text{V}_2\text{P}$ isomers, for solutions containing the oxoanion components in the $(\text{Mo} + \text{V})/\text{P} = (10 + 2):1$ ratio. Comparison between different total concentrations shows that a decrease in concentration gives a decrease in the pH stability range of the $\text{Mo}_{10}\text{V}_2\text{P}$ compositions as well. This is especially pronounced at the acidic end of the pH range, where the $\text{Mo}_{10}\text{V}_2\text{P}$ composition dissociates VO_2^+ and reconstitutes as $[\text{Mo}_{11}\text{VPO}_{40}]^{4-}$. This equilibrium decomposition of $\text{Mo}_{10}\text{V}_2\text{P}$ and $\text{Mo}_9\text{V}_3\text{P}$ compositions to $[\text{Mo}_{11}\text{VPO}_{40}]^{4-}$ with increasing acidity in the pH region where they become monoprotonated ($\text{pH} \approx 1$ and less) can also be discerned in the distribution diagrams of Figure 5 and 6. Similarly, Figure 5 shows that the $\text{Mo}_9\text{V}_3\text{P}$ compositions decompose to $[\text{Mo}_{10}\text{V}_2\text{PO}_{40}]^{5-}$ with increasing acidity in the pH region where they become protonated. The decomposition of Keggin molybdovanadophosphates, dissociating VO_2^+ and redistributing to lower vanadium-content Keggin species, is favoured by: (1) decreasing Keggin ion concentrations, favouring dissociative equilibria, (2) increasing acidity, and (3) increasing vanadium content in the Keggin composition. It is also favoured by (4) reduction of vanadium(V) to vanadium(IV), in which case VO^{2+} is dissociated.

Assignments of NMR Resonances to Mo₉V₃P Isomers

In the previous study,^[18] it proved possible to completely assign the ^{31}P and ^{51}V resonances of $\alpha\text{-}[\text{Mo}_{11}\text{VPO}_{40}]^{4-}$, of all five of the $\alpha\text{-Mo}_{10}\text{V}_2\text{P}$ isomers, and of the couple of $\beta\text{-Mo}_{10}\text{V}_2\text{P}$ isomers existing in detectable concentrations in the equilibrium solutions. The assignments of the resonances to the α -isomers relied on a number of factors:

- The ability to resolve the ^{31}P and ^{51}V resonances and to track them over pH
- Interpretations based on comparisons of the relative intensities of the resonances to the statistically predicted relative abundances of the α -isomers^[28]
- The expected relative magnitudes of the ^{51}V chemical shift changes of the different isomers in response to their protonation
- The expected relative $\text{p}K_{\text{a}}$ values of the monoprotonated anions
- The expected broader ^{51}V resonance line width of the α -(1,2) isomer with corner-sharing V-octahedra^[21]
- Correlations between the ^{31}P and ^{51}V resonances based on these factors

It did not prove possible to make a similar complete assignment of the detected ^{31}P and ^{51}V resonances of the individual $\text{Mo}_9\text{V}_3\text{P}$ isomers. The ^{51}V resonances proved too broad and overlapping, at 131.5 MHz, to be resolved and to be tracked over the pH range. The ^{31}P resonances of only six of the most abundant $\text{Mo}_9\text{V}_3\text{P}$ isomers could be resolved and tracked over pH, at 202.5 MHz (Figure 2). Nonetheless, partial assignments of the ^{31}P and ^{51}V resonances to structural motifs of the $\text{Mo}_9\text{V}_3\text{P}$ isomers did prove possible. These interpretations depended substantially on analogy to the more definitive assignments of the ^{31}P and ^{51}V resonances of the $\text{Mo}_{10}\text{V}_2\text{P}$ isomers. This analysis focused on the spectra of solutions with the oxoanion components in the $(\text{Mo} + \text{V})/\text{P} = (9 + 3):1$ ratio at $\text{pH} \geq 4.5$. The ^{31}P spectrum of such a solution (120 mM P) at $\text{pH} = 5.96$ at 25°C showed that about 87% of the phosphorus was present in the $\text{Mo}_9\text{V}_3\text{P}$ species, with the balance distributed in essentially equal amounts between the $\text{Mo}_{10}\text{V}_2\text{P}$ species and the $\text{Mo}_8\text{V}_4\text{P}$ species. (See Figure 8 and the discussion of the ^{31}P spectrum below.) At $\text{pH} \geq 4.5$, all the $\text{Mo}_{10}\text{V}_2\text{P}$ and $\text{Mo}_9\text{V}_3\text{P}$ isomers are fully deprotonated, so that protonation effects on their chemical shifts could be avoided when they were compared.

^{51}V NMR Spectra

The ^{51}V resonances of vanadium oxoanions have narrower line widths, and are therefore better resolved, at higher temperature. Our previous study^[18] determined that the relative abundances of the $\text{Mo}_{10}\text{V}_2\text{P}$ isomers are approximately the same at 25 and 90°C . This is also expected to be the case for the $\text{Mo}_9\text{V}_3\text{P}$ isomers. Consequently, our analysis of the ^{51}V resonances of the $[\text{Mo}_9\text{V}_3\text{PO}_{40}]^{6-}$ species focused on spectra of solutions at 90°C . However, even at this higher temperature, and with resolution enhancement algorithms, it was not possible to resolve the ^{51}V resonances of all the isomers.

The 13 α -isomers of the $[\text{Mo}_9\text{V}_3\text{PO}_{40}]^{6-}$ composition (Table 1) will, by symmetry, exhibit 30 potentially resolvable ^{51}V -NMR resonances. Table 4 shows the 30 inequivalent vanadium environments among the 13 α -isomers. Many of these inequivalent vanadium environments are obviously very similar, so it is expected that many of their resonances would have very close chemical shifts and are not resolved.

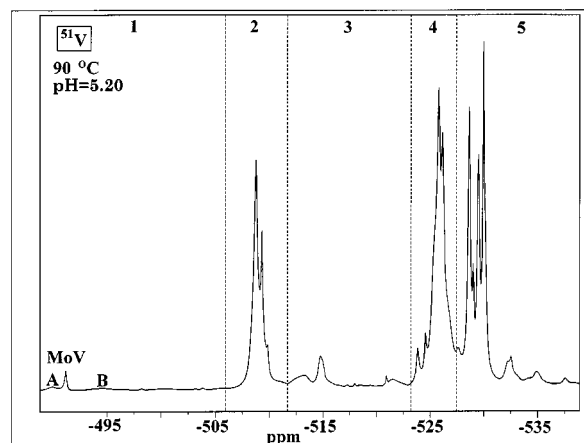


Figure 7. The ^{51}V spectrum of a solution containing the oxoanion components in the ratio $(\text{Mo} + \text{V})/\text{P} = (9 + 3):1$ (120 mM P) at 90°C , at which temperature the $\text{pH} = 5.20$. The chemical shift regions 1–5 are discussed in the text

Figure 7 shows the ^{51}V spectrum of a solution containing the oxoanion components in the ratio $(\text{Mo} + \text{V})/\text{P} = (9 + 3):1$ (120 mM P) at $\text{pH} = 5.20$ at 90°C . By analogy to the ^{51}V resonances of the α - $[\text{Mo}_{10}\text{V}_2\text{PO}_{40}]^{5-}$ isomers,^[18] five regions of the spectrum, divided as shown in Figure 7, were assigned to five distinct types of vanadium environments within the $[\text{Mo}_9\text{V}_3\text{PO}_{40}]^{6-}$ isomers, as described below.

α -1,4- $[\text{Mo}_{10}\text{V}_2\text{PO}_{40}]^{5-}$, the sole $\text{Mo}_{10}\text{V}_2\text{P}$ α -isomer in which the two vanadium octahedra are edge-sharing, is distinguished by the most downfield ^{51}V resonance of the $[\text{Mo}_{10}\text{V}_2\text{PO}_{40}]^{5-}$ isomers, 16 ppm downfield from the nearest other $[\text{Mo}_{10}\text{V}_2\text{PO}_{40}]^{5-}$ resonance, at $\delta = -509.75$ at 90°C . By analogy, region 2, at $\delta = -506$ to -512 in the $\text{Mo}_9\text{V}_3\text{P}$ spectrum at 90°C (Figure 7), is assigned to pairs of vanadium octahedra that are edge-sharing, but are separated from the third vanadium octahedron in the Keggin structure.

By analogy to the α -1,4- $[\text{Mo}_{10}\text{V}_2\text{PO}_{40}]^{5-}$ resonance's chemical shift being distinctly far downfield from the resonances of other $[\text{Mo}_{10}\text{V}_2\text{PO}_{40}]^{5-}$ isomers, the most downfield resonances of the $\text{Mo}_9\text{V}_3\text{P}$ isomers, in region 1, are assigned to isomers in which all three vanadium octahedra are mutually edge-sharing in a V_3O_{13} unit. The narrow resonance labelled MoV in Figure 7 is known to be that of the molybdovanadate species $[\text{Mo}_4\text{V}_2\text{O}_{19}]^{4-}$.^[16,17] In this region, there are two minor resonances, marked A and B, of $\text{Mo}_9\text{V}_3\text{P}$ species. However there is only one α - $\text{Mo}_9\text{V}_3\text{P}$ isomer (α -1,4,9) where all three vanadium octahedra are mutually edge-sharing. The furthest downfield resonance, A, is tentatively assigned to the vanadium atoms of α -1,4,9- $[\text{Mo}_9\text{V}_3\text{PO}_{40}]^{6-}$. The very broad resonance B might arise from a β -isomer in which all three vanadium octahedra are mutually edge-sharing. This could be the β -10,11,12 or the β -1,4,9 isomer, in which the mutually edge-sharing V_3O_{13} unit or a mutually edge-sharing Mo_3O_{13} unit, respectively, in the α -1,4,9 structure is rotated by $\pi/3$, or possibly both isomers.

Table 4. The 30 possible ^{51}V NMR resonances of the 13 $\alpha\text{-}[\text{Mo}_9\text{V}_3\text{PO}_{40}]^{6-}$ isomers. The VO_6 octahedra are shaded and the octahedron(s) responsible for the resonance is/are in dark colour. The table reports the statistically predicted relative intensities of the resonances and the regions of the spectrum in which the specific resonance is thought to appear (see Figure 7)

Polyhedral Structure	Designation	Statistical Abundance	Region	Polyhedral Structure	Designation	Statistical Abundance	Region
	$\alpha\text{-1,4,9}$	1.82 %	1		$\alpha\text{-1,2,8}$	3.63 %	4
	$\alpha\text{-1,2,3}$	1.82 %	4		$\alpha\text{-1,2,8}$	3.63 %	4
	$\alpha\text{-1,2,4}$	3.63 %	2		$\alpha\text{-1,2,8}$	3.63 %	5
	$\alpha\text{-1,2,4}$	3.63 %	3		$\alpha\text{-1,2,11}$	3.63 %	4
	$\alpha\text{-1,2,4}$	3.63 %	4		$\alpha\text{-1,2,11}$	3.63 %	4
	$\alpha\text{-1,2,6}$	3.63 %	2		$\alpha\text{-1,2,11}$	3.63 %	5
	$\alpha\text{-1,2,6}$	3.63 %	3		$\alpha\text{-1,2,10}$	3.64 %	4
	$\alpha\text{-1,2,6}$	3.63 %	4		$\alpha\text{-1,2,10}$	1.82 %	5
	$\alpha\text{-1,4,6}$	3.64 %	2		$\alpha\text{-1,5,8}$	1.82 %	5
	$\alpha\text{-1,4,6}$	1.82 %	5		$\alpha\text{-1,5,8}$	3.64 %	5
	$\alpha\text{-1,4,7}$	3.63 %	2		$\alpha\text{-1,5,7}$	3.63 %	5
	$\alpha\text{-1,4,7}$	3.63 %	2		$\alpha\text{-1,5,7}$	3.63 %	5
	$\alpha\text{-1,4,7}$	3.63 %	5		$\alpha\text{-1,5,7}$	3.63 %	5
	$\alpha\text{-1,4,8}$	3.63 %	2		$\alpha\text{-1,6,12}$	3.61 %	5
	$\alpha\text{-1,4,8}$	3.63 %	2				
	$\alpha\text{-1,4,8}$	3.63 %	5				

$\alpha\text{-1,2-}[\text{Mo}_{10}\text{V}_2\text{PO}_{40}]^{5-}$, the sole $\text{Mo}_{10}\text{V}_2\text{P}$ α -isomer in which the two vanadium octahedra are corner-sharing, exhibits the next most downfield ^{51}V resonance of the $[\text{Mo}_{10}\text{V}_2\text{PO}_{40}]^{5-}$ isomers, at $\delta = -526.10$ at 90°C . By analogy, region 4 at $\delta = -523$ to -527 in the $\text{Mo}_9\text{V}_3\text{P}$ spectrum at 90°C (Figure 7) is assigned to pairs of vanadium octahedra that are corner-sharing, but are separated from the third vanadium octahedron in the Keggin structure. The α -isomer with three mutually corner-sharing vanadium octahedra ($\alpha\text{-1,2,3}$) could be expected to have its resonance in this region (but see below).

The resonances in region 3, between region 2 of edge-sharing vanadium octahedra pairs and region 4 of corner-sharing vanadium octahedra pairs, are consequently assigned to individual vanadium octahedra that are positioned between the two others, edge-sharing with one and corner-sharing with the other. Since edge-sharing with another vanadium octahedron has such a strong downfield effect on the chemical shift, the two resonances that are

both the most downfield and the most intense within region 3 are reasonably assigned to these “in-between” vanadium octahedra in the $\alpha\text{-1,2,4}$ and $\alpha\text{-1,2,6}$ isomers. The more upfield and more minor resonances within region 3 may be the “in-between” vanadium octahedra in the β -isomers. It is also possible that the resonance of the $\alpha\text{-1,2,3}$ isomer (with *three* mutually corner-sharing vanadium octahedra) may be downfield of region 4, in region 3.

The $\alpha\text{-1,2-}[\text{Mo}_{10}\text{V}_2\text{P}]$ isomer is also unique among the $\alpha\text{-}[\text{Mo}_{10}\text{V}_2\text{P}]$ isomers in having a distinctively broad resonance line width.^[18] This is expected for corner-sharing vanadium octahedra, as revealed by Leparulo-Loftus and Pope's study of isostructural tungstovanadates, including α -Keggin decatungstodivanadophosphate isomers, and is supported by the theoretical explanation provided in that report.^[21] It also was a key factor, but not an isolated factor, in the complete assignment of the ^{51}V resonances of the $\text{Mo}_{10}\text{V}_2\text{P}$ isomers. By an extensive evaluation of line widths of the resonances in the major intensity regions 2, 4, and 5 by line shape

Table 5. The statistically predicted relative abundance of the α -[Mo₁₀V₂P₄₀]⁵⁻ isomers and their actual relative abundance by ⁵¹V resonance intensities. The statistically predicted relative intensities of groups of ⁵¹V resonances of the α -[Mo₉V₃P₄₀]⁶⁻ isomers, grouped by type of vanadium environment, and the actual relative intensities among the regions of the spectrum assigned to these groups, as shown in Figure 7. The last column gives, as a percentage, the disparity between the actual relative intensities and those statistically predicted

Isomers	Statistical abundance	Integral ⁵¹ V	Disparity %
Mo ₁₀ V ₂ P			
α -1,4 (pair of edge-sharing V)	18.2%	13.3%	73%
α -1,2 (pair of corner-sharing V)	18.2%	23.3%	128%
α -1,5 + α -1,6 + α -1,11 (separated V)	63.7%	63.3%	99%
Mo ₉ V ₃ P			
Region 1 (edge-sharing V ₃ O ₁₃ units)	1.8%	0.7%	39%
Region 2 (pairs of edge-sharing V)	25.4%	20.5%	81%
Region 3 (V edge-sharing to another V and corner-sharing to a third V)	7.3%	4.9%	67%
Region 4 (pairs of corner-sharing V)	27.2%	37.0%	136%
Region 5 (V separated from other V)	38.1%	37.0%	97%

analysis, the resonances in region 4 were determined to have broader line widths than the resonances in these other regions. This further supports the assignment of the resonances in region 4 to corner-sharing vanadium octahedra. The resonances in region 3, assigned to the “in-between” vanadium octahedrons that are corner-sharing with another vanadium octahedron, have visually broad line widths, as seen in Figure 7.

The three α -Mo₁₀V₂P isomers, and the one detected β -Mo₁₀V₂P isomer with separated vanadium octahedra have resonances with narrow line widths at $\delta = -528$ to -529 at 90 °C.^[18] By analogy, region 5 in the Mo₉V₃P spectrum, upfield of $\delta = -527$ at 90 °C (Figure 7) and comprising narrow resonances closely grouped between $\delta = -528$ and -530 , is assigned to the isolated vanadium octahedrons within the Mo₉V₃P isomers.

This assignment of the resonances by chemical shift region to five different types of vanadium environments found in the Mo₉V₃P isomers accords well with the expected relative abundances of these environments in the α -isomers. The statistically predicted relative abundances of the 30 inequivalent vanadium environments among the α -isomers are listed in Table 4. A direct comparison of the resonance intensities, integrated region-by-region, with these statistically predicted relative abundances of the different types of vanadium environments among the α -isomers is complicated by two factors. First, this analysis ignores the presence of β -isomers. Second, it assumes that the 13 α -isomers are all of equal stability, so their distribution is governed solely by the statistics of their structural degeneracies. The results of this comparison are presented below after these complicating factors are discussed.

As discussed in the introduction, β structures become more likely as molybdenum(VI) in the parent Keggin molybdophosphate ion, [Mo₁₂PO₄₀]³⁻, is increasingly substituted by vanadium(V). In the previous work, no β -isomer of [Mo₁₁VPO₄₀]⁴⁻ was detected, and about 10% of the total vanadium in the Mo₁₀V₂P species was present in β -isomers.^[18] Therefore, more than 10% of the total vanadium in the Mo₉V₃P species is expected to be present in β -isomers in this case. The ³¹P spectrum (Figure 8) of the solution, at 25 °C, whose ⁵¹V spectrum, at 90 °C, is shown in Figure 7,

indicates that about 17% of the P in the Mo₉V₃P species is present in β -isomers. (See discussion below.)

The ⁵¹V resonances of similar vanadium environments (edge- or corner-sharing with another vanadium octahedron, separated, etc.) are expected to have similar chemical shifts whether in an α - or a β -isomer, and to appear in the same region of the spectrum. This is the case for the ⁵¹V resonances of the deprotonated Mo₁₀V₂P isomers.^[18] In the ⁵¹V NMR spectrum at 90 °C, two β -[Mo₁₀V₂P₄₀]⁵⁻ were detected. One, assigned to the β -4,11 isomer with separated vanadium octahedra, has the chemical shift $\delta = -528.8$ and is overlapped by the resonances of the α -isomers with separated vanadium octahedra. The other, assigned to the β -4,10 isomer with corner-sharing vanadium octahedra, the assignment being based in part on its relatively broad line width, characteristic of corner-sharing vanadium octahedra, has its chemical shift at $\delta = -526.7$, nearest to the α -1,2-[Mo₁₀V₂P₄₀]⁵⁻ isomer with corner-sharing vanadium octahedra. The chemical shifts for these β -isomers are within the designated regions (Figure 7) for separated (region 5) and corner-sharing (region 4) vanadium octahedra.

Accordingly, the presence of β -isomers should not compromise the assignments of the spectral regions to the various types of vanadium environments. However, to the extent that certain structural relationships among the vanadium octahedra (edge- or corner-sharing with another vanadium, separated, etc.) are more conducive to stabilising β -structures than others, the distribution of the types of vanadium environments determined by resonance integration region-by-region will be skewed by their distribution among only the α -isomers.

The previous study revealed that the α -isomers of [Mo₁₀V₂P₄₀]⁵⁻ are not of equal stability.^[18] While their relative abundances in solution approximate their statistically predicted relative abundances, there are some significant deviations. Table 5 lists the α -Mo₁₀V₂P isomers with their type of vanadium environment and compares the statistically predicted relative abundances of the types of vanadium environments with their relative abundances in the deprotonated α -isomers, (only) determined by their resonance intensities. The α -1,4 isomer, with edge-sharing vanadium octahedra, is substantially less abundant than predicted by

statistics. In contrast, the α -1,2 isomer, with corner-sharing vanadium octahedra, is substantially more abundant than predicted by statistics. The total abundance of the remaining α -isomers, with spread (separated) vanadium octahedra, closely agrees with their total statistically predicted abundance.

Table 5 also lists the types of vanadium environments of the $\text{Mo}_9\text{V}_3\text{P}$ isomers, assigned by spectral region, and compares the statistically predicted relative abundances of these types of vanadium environments among the α - $\text{Mo}_9\text{V}_3\text{P}$ isomers, with their relative abundances determined by region-by-region integration of the spectrum shown in Figure 7. This comparison shows that the relative abundances of the types of vanadium environments approximate their statistically predicted relative abundances, but with discrepancies directly analogous to those found for the $\text{Mo}_{10}\text{V}_2\text{P}$ isomers. The abundance of pairs of edge-sharing vanadium octahedra (region 2) is substantially less than statistically predicted. The abundance of pairs of corner-sharing vanadium octahedra (region 4) is substantially greater than statistically predicted. The abundance of isolated vanadium octahedra separated from others (region 5) closely agrees with the statistics.

The abundance of isomers in which all three vanadium octahedra are mutually edge-sharing in a V_3O_{13} unit (region 1) is even more depressed relative to the statistically predicted abundance of the α -1,4,9 isomer than the abundance of pairs of edge-sharing vanadium octahedra (region 2) relative to their statistical prediction. This appears directionally consistent, but it must be noted that it is difficult to obtain accurate integrated intensities for such weak resonances as in region 1.

In view of this analogy to the relative abundances of the $\text{Mo}_{10}\text{V}_2\text{P}$ isomers, the assignment of the ^{51}V resonances of the $\text{Mo}_9\text{V}_3\text{P}$ isomers by chemical shift region to the different types of vanadium environments appears well supported by the region-by-region integration of their resonance intensities.

^{31}P -NMR Spectra

The ^{31}P -NMR resonances of $\text{Mo}_9\text{V}_3\text{P}$ species proved to be difficult to assign to specific isomers. Our examination of the ^{31}P -NMR resonances of the Keggin $[\text{Mo}_9\text{V}_3\text{PO}_{40}]^{6-}$ species focused on the spectra of solutions at 25 °C. Contrary to their ^{51}V -NMR resonances, the ^{31}P resonances of these Keggin oxoanions have narrower line widths and are better resolved at 25 °C than at higher temperatures.

Figure 8 shows the ^{31}P spectrum of the same solution, at 25 °C, whose ^{51}V spectrum at 90 °C is shown in Figure 7. (Its pH at 25 °C is 5.96.) The ^{31}P spectrum allows an assessment of the relative amounts of the $\text{Mo}_{(12-x)}\text{V}_x\text{P}$ compositions present. Resonances can be readily sorted by x of the $\text{Mo}_{(12-x)}\text{V}_x\text{P}$ compositions, when their relative intensities in solutions of various Mo/V ratios are observed.^[18] Region A in Figure 8 contains resonances of $\text{Mo}_8\text{V}_4\text{P}$ species, which comprise approx. 6.4% of the total phosphorus in solution. Some minor $\text{Mo}_8\text{V}_4\text{P}$ resonances, further upfield among the resonances in region B of Figure 8, are unresolved. On the

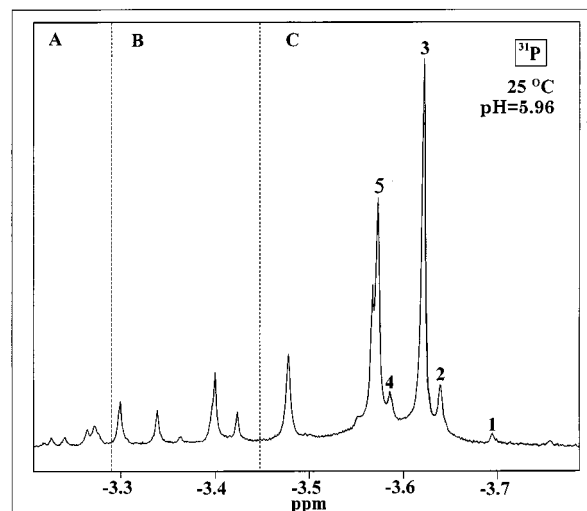


Figure 8. The ^{31}P spectrum of the same solution whose ^{51}V spectrum is shown in Figure 7, but at 25 °C, at which temperature the pH is 5.96. The chemical shift regions, A, B, and C are discussed in the text

basis of the overall composition of the solution, corresponding to the average composition $\text{Mo}_9\text{V}_3\text{P}$, it is concluded that an essentially equal amount of the total phosphorus in the solution is present as $\text{Mo}_{10}\text{V}_2\text{P}$ species, whose resonances are among the $\text{Mo}_9\text{V}_3\text{P}$ resonances in region C of Figure 8.^[18] Consequently, about 87% of the total phosphorus in this solution is present in $\text{Mo}_9\text{V}_3\text{P}$ species.

A partial assignment of the ^{31}P resonances of $\text{Mo}_9\text{V}_3\text{P}$ species proved possible by analogy to what was learned previously from the full assignment of the ^{31}P resonances of the $\text{Mo}_{10}\text{V}_2\text{P}$ isomers.^[18] The resonances of the α - and β - $[\text{Mo}_{10}\text{V}_2\text{PO}_{40}]^{5-}$ isomers appear in separate chemical shift groups. This can be seen in Figure 2 from the chemical shift vs. pH curves of the $\text{Mo}_{10}\text{V}_2\text{P}$ species at pH > 3 where all the species are completely deprotonated. The resonances of the five α -isomers (all within the three resolved resonances labelled b, c, and d in Figure 2) appear closely grouped at distinctly higher field than the resonances detected for the two β -isomers (e and f in Figure 2), which also have a broader spread in chemical shifts. Figure 2 also shows that, at pH > 5 where the $\text{Mo}_9\text{V}_3\text{P}$ species are completely deprotonated, four of the six most intense ^{31}P resonances are closely grouped in the same chemical shift region as the resonances of the five α - $[\text{Mo}_{10}\text{V}_2\text{PO}_{40}]^{5-}$ isomers. (Only the most intense phosphorus resonances are plotted in Figure 2, as only they could be tracked as a function of pH as the various resonances converged and diverged.) These four high-field, more intense $\text{Mo}_9\text{V}_3\text{P}$ resonances, and the minor resonances in the same chemical shift region are confidently assigned to α - $[\text{Mo}_9\text{V}_3\text{PO}_{40}]^{6-}$ isomers.

The most downfield $[\text{Mo}_9\text{V}_3\text{PO}_{40}]^{6-}$ resonance plotted in Figure 2, which is downfield of even the most downfield detected β - $[\text{Mo}_{10}\text{V}_2\text{PO}_{40}]^{5-}$ resonance, appears on this basis to be a β - $[\text{Mo}_9\text{V}_3\text{PO}_{40}]^{6-}$ isomer. Similarly, the most downfield resonance in region C of Figure 8 has a chemical shift between the two detected β - $[\text{Mo}_{10}\text{V}_2\text{PO}_{40}]^{5-}$ resonances, but its intensity, greater than that of any resonance

in region B, is more consistent with an α -isomer. There is probably no distinct chemical shift border between the resonances of the 13 α -isomers and 43 β -isomers of $\text{Mo}_9\text{V}_3\text{P}$ composition.

To get an approximation of the relative amounts of α - and β - $\text{Mo}_9\text{V}_3\text{P}$ isomers, we considered the resonances in region C to be α - $\text{Mo}_9\text{V}_3\text{P}$ isomers, subtracting the contribution from $\text{Mo}_{10}\text{V}_2\text{P}$ isomers, and the resonances in region B to be β - $\text{Mo}_9\text{V}_3\text{P}$ isomers. The integrated resonance intensities over these regions indicate approximately 17% β - and 83% α - $\text{Mo}_9\text{V}_3\text{P}$ isomers. Table 1 lists two columns of statistically predicted abundances of the α - $\text{Mo}_9\text{V}_3\text{P}$ isomers. The first (1) gives the statistically predicted distribution of the α -isomers among the total α -isomers, as if only α -isomers were present (total 100%). The second (2) gives the statistically predicted distribution of the α -isomers among the total α -isomers, corrected for only 83% of the total phosphorus being present in α -isomers (total 83%). This second "predicted relative abundance" distribution was used for comparing individual ^{31}P resonance intensities, as a percentage of the total intensity of the ^{31}P resonances of $\text{Mo}_9\text{V}_3\text{P}$ (regions B + C, corrected for the $\text{Mo}_{10}\text{V}_2\text{P}$ contribution), to the predicted percentage relative abundance of the isomers (see below).

A partial assignment of the ^{31}P resonances in region C of Figure 8 to specific α - $[\text{Mo}_9\text{V}_3\text{PO}_{40}]^{6-}$ isomers is based on their relative intensities and a trend revealed by the assignment of the ^{31}P resonances of the α - $[\text{Mo}_{10}\text{V}_2\text{PO}_{40}]^{5-}$ isomers.^[18] The ^{31}P resonances of the unprotonated α - $[\text{Mo}_{10}\text{V}_2\text{PO}_{40}]^{5-}$ isomers reflect, in chemical shift order from upfield to downfield, decreasing polarity in the charge distribution surrounding the phosphorus. The more the vanadium atoms are separated in the Keggin structure, decreasing the charge polarity, the lower the field of the chemical shift. On this same basis, the α - $[\text{Mo}_9\text{V}_3\text{PO}_{40}]^{6-}$ isomers have been ordered in Table 1, from top-to-bottom, in the expected chemical shift order, from upfield to downfield.

The α - $[\text{Mo}_9\text{V}_3\text{PO}_{40}]^{6-}$ isomer with the most unbalanced charge distribution, expected to be most upfield, is the α -1,4,9 isomer (at the top of Table 1), with a predicted relative abundance of 1.5%. The most upfield significant resonance in Figure 8, labelled 1, contains 0.8% of the total phosphorus of regions B and C. The next resonance, labelled 2 in Figure 8, contains 5.4% of the total phosphorus in regions B and C. The α -1,2- and α -1,5- $[\text{Mo}_{10}\text{V}_2\text{PO}_{40}]^{5-}$ species also appear at this chemical shift,^[18] unresolved, and contribute to about half of this integrated relative intensity. Thus, approx. 2.7% of the total phosphorus intensity may be assigned to the α -1,2,3 isomer. A comparison with the two most unbalanced charged α - $[\text{Mo}_{10}\text{V}_2\text{PO}_{40}]^{5-}$ isomers shows that the integral of α -1,4,9 should be underestimated and α -1,2,3 overestimated. One would expect to find these two resonances well separated, since vanadium atoms are connected by sharing oxygen either in a corner or on an edge.

The next downfield, resolved resonance in Figure 8, labelled 3, which is the most intense resonance in the spectrum, has a total relative intensity of approx. 31% over re-

gions B and C. This resonance overlaps the resonances of α -1,6- and α -1,11- $[\text{Mo}_{10}\text{V}_2\text{PO}_{40}]^{5-}$, which should contribute approx. 2.7% to this integrated relative intensity, leaving approx. 28% for $\text{Mo}_9\text{V}_3\text{P}$ species. The three α - $\text{Mo}_9\text{V}_3\text{P}$ isomers which appear next in the charge distribution order (Table 3), α -1,2,4, α -1,2,6 and α -1,4,8, have very similar charge distributions (unique in having all vanadium octahedra connected in series, but not all mutually connected as in the preceding two isomers in Table 1). Their predicted statistical abundance of 27.3% makes assignment of the resonance labelled 3 plausible. Examination of this resonance by curve fitting shows that it is composed of two resonances in a 2:1 ratio. According to charge distribution, the α -1,2,4 and α -1,2,6 isomers with a pair of edge-sharing vanadium octahedra and a third corner-sharing vanadium octahedron are more alike in charge than the α -1,4,8 isomer in which the third vanadium octahedron is separated from the other two.

The next downfield resonance (labelled 4 in Figure 8) is expected to be that of the α -1,4,6 isomer. Its relative intensity over regions B and C, 5.2%, agrees well with the predicted statistical abundance of 4.5%. The still next downfield resonance (labelled 5 in Figure 8), with a relative intensity of approx. 20% of the total phosphorus in regions B and C, agrees well with the sum of the predicted statistical abundances (18.2%) of the next two expected α -1,2,8 and α -1,4,7 isomers.

Beyond this, the remaining ^{31}P resonances could not be assigned to $\text{Mo}_9\text{V}_3\text{P}$ species with any confidence. At increasingly downfield chemical shift, above $\delta = -3.5$, it becomes less and less certain whether the resonances arise from α -isomers or β -isomers or both. We can note that the α -1,6,12- $[\text{Mo}_9\text{V}_3\text{PO}_{40}]^{6-}$ isomer, with the most balanced internal charge distribution among the α - $\text{Mo}_9\text{V}_3\text{P}$ species, is expected to have the most downfield chemical shift among the α - $[\text{Mo}_9\text{V}_3\text{PO}_{40}]^{6-}$ species. With a very low predicted statistical abundance (Table 1), however, its resonance could not be clearly assigned.

Experimental Section

Concentrated Molybdovanadophosphate Solutions and Solids: Molybdovanadophosphate sodium salt solutions were prepared by the method developed at Catalytica.^[22] Free molybdovanadophosphoric acid solutions were prepared by the method developed by Onoda and Otake,^[23] with modifications.^[22] The solutions 0.30 M $\{\text{Na}_5\text{Mo}_{10}\text{V}_2\text{PO}_{40}\}$, 0.317 M $\{\text{H}_{4.9}\text{Mo}_{10.1}\text{V}_{1.9}\text{PO}_{40}\}$, 0.10 M $\{\text{Na}_4\text{Mo}_{11}\text{VPO}_{40}\}$, and 0.30 M $\{\text{H}_4\text{Mo}_{11}\text{VPO}_{40}\}$, and the solids $\{\text{Na}_5\text{Mo}_{10}\text{V}_2\text{PO}_{40}\} \cdot 13.6 \text{ H}_2\text{O}$, $\{\text{H}_5\text{Mo}_{10}\text{V}_2\text{PO}_{40}\} \cdot 10.1 \text{ H}_2\text{O}$, $\{\text{Na}_4\text{Mo}_{11}\text{VPO}_{40}\} \cdot 12.4 \text{ H}_2\text{O}$, and $\{\text{H}_4\text{Mo}_{11}\text{VPO}_{40}\} \cdot 21.5 \text{ H}_2\text{O}$ are those whose preparations were previously described.^[18] A solution of 0.30 M $\{\text{Na}_5\text{HMo}_9\text{V}_3\text{PO}_{40}\}$, also used in the present studies, was prepared by neutralisation of 0.30 M $\{\text{Na}_3\text{H}_3\text{Mo}_9\text{V}_3\text{PO}_{40}\}$. These solutions were prepared as described below. Raw material sources were the same as for the previously reported preparations.^[18]

Solution of 0.30 M $\{\text{Na}_3\text{H}_3\text{Mo}_9\text{V}_3\text{PO}_{40}\}$: In a 12 L Morton flask equipped with an electric heating mantle, efficient reflux condenser, and high torque overhead mechanical stirrer, granular V_2O_5 (4.50

mol, 818.46 g) was suspended in 3.5 L of distilled water, and the mixture was heated to about 60 °C. Granular anhydrous Na₂CO₃ (4.50 mol, 476.95 g) was slowly added in portions to the rapidly stirred mixture, causing CO₂ liberation and dissolution of the V₂O₅ to give an essentially homogeneous solution. The solution was heated at reflux for 1 h. The solution was then dark blue-green due to dissolved V^{IV} which was originally present in the V₂O₅. Approximately 1 mL of 30% H₂O₂ was added dropwise, causing the dark blue-green colour to fade, leaving a slightly turbid, pale-tan sodium metavanadate solution. The solution was maintained at reflux for an additional 60 min to ensure the decomposition of excess peroxide and it was then cooled to room temp. The solution was filtered to remove the small amount (< 0.2 g) of brown solid, which contained almost all the iron and silica impurities originally present in the V₂O₅. The clear sodium metavanadate solution (orange coloured owing to small amounts of decavanadate species present at this very high vanadate concentration) was then returned to the Morton flask, diluted with 4.0 L of distilled water; then MoO₃ (27.00 mol, 3886.38 g) was added with rapid stirring. The mixture was heated to about 60 °C and H₃PO₄ (3.00 mol, 344.25 g, 85.4% w/w) was added. The mixture was heated at reflux and thereby converted into a clear, dark, burgundy-red solution. After 3 h at reflux, the homogenous solution was cooled to room temp and was volumetrically diluted with distilled water to a total volume of 10.00 L, giving 0.30 M {Na₃H₃PMo₉V₃O₄₀}.

Solution of 0.30 M {Na₅HMo₉V₃PO₄₀}: Granular Na₂CO₃ (0.15 mol, 15.90 g) was slowly added to {Na₃H₃PMo₉V₃O₄₀} (0.15 mol, 0.500 L, 0.30 M) with rapid stirring. The resulting solution was boiled for 1.5 h, cooled to room temp, and volumetrically diluted with distilled water to 0.500 L, giving 0.30 M {Na₅HMo₉V₃PO₄₀}.

Solutions for Potentiometric and Quantitative NMR Studies: Stock solutions of the components (HCl, Na₂MoO₄, NaVO₃, and NaH₂PO₄) were prepared as previously described, from the same source materials.^[13,18] The solutions for the potentiometric and NMR studies were prepared by mixing of the stock solutions of the components, from the concentrated molybdovanadophosphate solutions (listed above), and/or from the solid Keggin molybdovanadophosphoric acids and sodium salts (listed above) in the same manner as previously described.^[18] Boiled distilled water was used to prepare all the solutions. After the components were mixed, the molybdovanadophosphate solutions required up to 24 h at 25 °C to reach equilibrium. For measurements at 90 °C, see ref.^[18]

Ionic Medium: The pH potentiometry at 25 °C and the NMR studies at 25 °C and 90 °C were all conducted on solutions of the ionic 0.6 M Na(Cl), to maintain constant activity coefficients. Since anion equilibria are studied, the cation concentration in the ionic medium was kept constant, 0.600 M Na⁺, and the Cl[−] concentration was varied to provide the balance of counteranions not provided by the molybdate, vanadate, and phosphate oxoanion species. This is the same medium referred to in previous studies as 0.6 M Na(Cl).

pH Potentiometry: Titrations were conducted at 25.0 ± 0.1 °C with an automated potentiometric titrator. Free H⁺ concentrations were determined by measurement of the EMF of the cell given below, with an Ingold type 201-NS glass electrode, an Ag/AgCl reference electrode prepared according to Brown,^[24] and a Wilhelm bridge.^[25] Cell: − Ag,AgCl | 0.6 M NaCl || equilibrium solution | glass electrode +

The free H⁺ concentration was calculated from the measured EMF, *E* (in mV), by Equation (3), where the last term is the liquid junction potential in acid solutions for the 0.6 M Na(Cl) medium and the Wilhelm-type bridge used.

$$E = E_0 + 59.157 \log [\text{H}^+] - 76 [\text{H}^+] \quad (3)$$

The constant *E*₀ was determined before and after each titration with separate solutions of known [H⁺]. A fluoropolymer-encased magnetic bar was used to stir the solution in the titration vessel. The solution was protected from atmospheric carbon dioxide by a stream of argon gas. The argon was sparged through 10% NaOH solution to remove any acid impurities, 10% H₂SO₄ solution to remove any alkaline impurities, and, finally, a 0.6 M NaCl medium before introduction to the titration vessel.

pH Potentiometric Data: A total of 42 titrations covering the ranges of pH from 1.3 to 5.2, Mo/V ratios from 2 to 22, and (Mo + V)/P ratios from 11.5 to 15.4 were performed, and 187 selected points were used in the calculations. The solid lines in Figure 1 show the EMF titrations over (Mo/V) vs. pH space, and show that the titrations were done at constant pH with varying Mo/V ratios, at a constant Mo/V ratio with varying pH, and at simultaneously varied pH and Mo/V ratio. The total concentration of phosphorus was varied between 8 and 20 mM. To confirm that solutions reached equilibrium, pH titrations were done in both directions, acidic towards neutral and neutral towards acidic. The titration data used in the calculations were restricted to Mo/V ratios greater than 3.8 (corresponding to *x* ≤ 2.5 in the average Keggin composition [Mo_{12−*x*}V_{*x*}PO₄₀]^{(3+*x*)−}), to avoid solutions containing Mo₈V₄P anions. The data used in the calculations were also restricted to pH > 1.3, as data from titrations at lower pH values were not considered accurate enough.

NMR Measurements: The ³¹P- and ⁵¹V-NMR measurements were obtained on a Bruker AM500 spectrometer at 202.5 and 131.6 MHz, respectively. The probe temperature was thermostatted at 25.0 ± 0.5 °C or 90.0 ± 1.0 °C. The field frequency stabilisation was locked to deuterium by insertion of the 8 mm sample tubes into 10 mm tubes containing D₂O. The samples were spinning in all experiments.

The spin-lattice relaxation times (*T*₁) were evaluated with the Bruker software inversion recovery method and were determined for the different Keggin species to approx. 30 s for ³¹P and just a few ms for ⁵¹V. For determining the relative abundances of species from their resonance intensities, spectra were recorded quantitatively with the relaxation delay set to at least 5·*T*₁, and the free induction decay (FID) was multiplied by an exponential line-broadening function (LB = 1), with the Bruker software, to improve the signal/noise ratio. A Gaussian-Lorentzian double apodization was applied to the FID, also with the Bruker software, to enhance resolution to obtain more accurate chemical shifts of overlapping resonances. Chemical shifts are reported relative to external VOCl₃ and external 85% H₃PO₄, with positive chemical shifts (δ) corresponding to higher frequency.

In acid solutions the α-[Mo₁₁VPO₄₀]^{4−} ion was used as internal ³¹P and ⁵¹V chemical shift standard to determine the chemical shifts with high accuracy and precision. In the more neutral solutions, the chemical shifts of the fully deprotonated [Mo₁₀V₂PO₄₀]^{5−} isomers had a constant “plateau” vs. pH and could be used as internal ³¹P and ⁵¹V chemical shift standards. The ³¹P chemical shifts are dependent on the concentration of Keggin ions, and 10 mM Keggin ions was used as the reference state for chemical shifts.^[18]

NMR solutions were collected from titrations and from separately prepared solutions (“point solutions”) corresponding to points in a hypothetical pH titration. After equilibration, the pH values in these point solutions were measured with a combination electrode, ORION Research 81-03 ROSS or INGOLD U402-M6-S7/100. The

electrodes were calibrated with solutions of known $[H^+]$ in 0.6 M NaCl. Due to the long relaxation time of ^{31}P resonances in Keggin species, the phosphorus concentrations were sometimes as high as 120 mM, which improves the signal/noise ratio in the spectra and facilitates the determination of chemical shifts with fewer scans.

NMR Data for the Calculations: Integrals from 44 NMR spectra ($0.44 < pH < 4.78$), shown with as \square in Figure 1, and 67 shift values from different spectra ($0 < pH < 6.13$) were used in the calculations. The total concentration of phosphorus was varied between 8 and 60 mM for integral data and between 8 and 120 mM for chemical shift data. Mo_8V_4P species appear in acid solutions with a Mo/V ratio of 3 ($x = 3$ in the average Keggin ion composition). NMR data used in the calculations were, in the same way as titration data, restricted to Mo/V ratios above 3.8, to avoid solutions containing Mo_8V_4P anions, and to thereby simplify the calculations.

The ^{31}P resonances are much better resolved than the ^{51}V resonances at 25 °C. Consequently, we mainly used the integral data from ^{31}P spectra, and not from ^{51}V spectra, in the calculations. In the more neutral solutions, however, the ^{31}P resonances were severely overlapped, so that it was not possible to obtain reliable integral values. For this reason, the NMR data used in the calculations were restricted to those obtained at $pH \leq 4.8$.

Computer Programs: Resonance intensities were computed by integration with the Bruker software, or, for overlapping resonances, by line shape analysis with the programs NMRi,^[26] UXNMR/P version 1.1, and WIN-NMR version 950901.0, with the chemical shifts determined by resolution enhancement (see above) as input. Using these programs, it is possible to obtain integral values with errors less than 10%. The mathematical analysis of combined $[H^+]$ -EMF data, and ^{31}P -NMR shift and integral data, was accomplished with the least-squares program LAKE.^[1] LAKE is capable of treating multimethod data simultaneously; this considerably refines the equilibrium analysis. Compositions, (p, q, r, s), and formation constants, $\beta_{p,q,r,s}$ are varied so that the error squares sum, $U = \sum (W_i \Delta A_i)^2$ is minimised. The complex, or set of complexes, with the lowest U value forms the model that best explains the experimental data. A_i can be either the total concentration of components, free species concentrations, NMR peak integrals, chemical shifts or a combination of these. W_i are weighting factors that are subjectively set to give different types of data appropriate contributions to the results. In the present study, we used weighting factors that give NMR peak integrals and shift values a predominant contribution to the sum of residuals. Calculation and plotting of distribution diagrams were performed with the program SOLGAS-WATER.^[27]

Acknowledgments

Financial support from Catalytica Inc. and the Swedish Natural Science Research Council (NFR) for the work at University of Umeå is hereby gratefully acknowledged.

^[1] N. Ingri, I. Andersson, L. Pettersson, A. Yagasaki, L. Andersson, K. Holmström, *Acta Chem. Scand.* **1996**, *50*, 717–734.

^[2] The ionic formulae of these Keggin anions are more commonly written as $[H_2PMo_{12-x}V_xO_{40}]^{(3+x-2)-}$. We usually denote the

composition of a solution species by the stoichiometric integers of the components used in our potentiometric study of its equilibrium formation. We also find it convenient to use our standard order – H, Mo, V, P – when writing ionic formulae.

- ^[3] C. L. Hill, C. M. Prosser-McCarthy, *Coord. Chem. Rev.* **1995**, *143*, 407–455.
- ^[4] J. H. Grate, D. R. Hamm, S. Mahajan, in: *Polyoxometallates: From Platonic Solids to Anti-retroviral Activity* (Eds.: M. T. Pope, A. Müller), Kluwer, Dordrecht, **1994**, pp. 281–305; J. H. Grate, D. R. Hamm, S. Mahajan, in: *Catalysis of Organic Reactions* (Eds.: J. R. Kosak, T. A. Johnson) Marcel Dekker, New York, **1984**, chapter 16, p. 213; International Applications published under the Patent Cooperation Treaty, Publication Numbers, WO 91/13851, WO 91/13853, and WO 91/13854, published 19 September, **1991**.
- ^[5] J. F. Keggin, *Nature* **1933**, *131*, 908–909; *Proc. Roy. Soc., Ser. A* **1934**, *144*, 75–100.
- ^[6] L. C. W. Baker, J. S. Figgis, *J. Am. Chem. Soc.* **1970**, *92*, 3794–3797.
- ^[7] M. T. Pope, *Heteropoly and Isopoly Oxometallates*; Springer-Verlag, New York, **1983**, pp. 23–27.
- ^[8] A. Tézé, J. Canny, L. Gurban, R. Thouvenot, G. Hervé, *Inorg. Chem.* **1996**, *35*, 1001–1005.
- ^[9] L. Pettersson, B. Hedman, I. Andersson, N. Ingri, *Chem. Scr.* **1983**, *22*, 254–264.
- ^[10] L. Pettersson, B. Hedman, A.-M. Nenner, I. Andersson, *Acta Chem. Scand* **1985**, *A 39*, 499–506.
- ^[11] K. Elvingsson, M. Fritzsche, D. Rehder, L. Pettersson, *Acta Chem. Scand.* **1994**, *48*, 878–885.
- ^[12] A. Yagasaki, I. Andersson, L. Pettersson, *Inorg. Chem.* **1987**, *26*, 3926–3933.
- ^[13] A. Selling, I. Andersson, L. Pettersson, C. M. Schramm, S. L. Downey, J. H. Grate, *Inorg. Chem.* **1994**, *33*, 3141–3150.
- ^[14] L. Pettersson, I. Andersson, L.-O. Öhman, *Inorg. Chem.* **1986**, *25*, 4726–4733. This study was carried out in 3.0 M NaClO₄, but the speciation is essentially the same as in 0.6 M NaCl (ref.^[15]).
- ^[15] L. Pettersson, I. Andersson, manuscript in preparation.
- ^[16] O. W. Howarth, L. Pettersson, I. Andersson, *Chem. Soc. Dalton Trans.* **1989**, 1915–1923.
- ^[17] O. W. Howarth, L. Pettersson, I. Andersson, *Chem. Soc. Dalton Trans.* **1991**, 1799–1812.
- ^[18] L. Pettersson, I. Andersson, A. Selling, J. H. Grate, *Inorg. Chem.* **1994**, *33*, 982–993.
- ^[19] L. Pettersson, in: *Polyoxometallates: From Platonic Solids to Anti-retroviral Activity* (Eds.: M. T. Pope, A. Müller), Kluwer, Dordrecht, **1994**, pp. 27–40.
- ^[20] Y. Jeannin, M. Fournier, *Pure Appl. Chem.* **1987**, *59*, 1529–1548.
- ^[21] M. A. Leparulo-Loftus, M. T. Pope, *Inorg. Chem.* **1987**, *26*, 2112–2120.
- ^[22] J. H. Grate, D. R. Hamm, R. J. Saxton, Internations Patent Application Publication Number WO 91/13681, 1991; J. H. Grate, *J. Mol. Catal. A* **1996**, *114*, 93–101.
- ^[23] T. Onoda, M. Otake, U.S. Patent 4,156,574, 1979.
- ^[24] A. S. Brown, *J. Am. Chem. Soc.* **1934**, *56*, 646–647.
- ^[25] W. Forsling, S. Hietanen, L.-G. Sillén, *Acta Chem. Scand.* **1952**, *6*, 901–909.
- ^[26] C. L. Dumoulin, G. C. Levy, *J. Mol. Struct.* **1984**, *113*, 299–310.
- ^[27] G. Eriksson, *Anal. Chim. Acta* **1979**, *112*, 375–383.
- ^[28] The statistically predicted relative abundances correspond to the α isomers' degeneracies, and are reported herein as percentages of the total of their degeneracies. The degeneracy of each isomer equals the number of ways x vanadium can be substituted for x molybdenum in the parent $T_d \alpha-[Mo_{12}PO_{40}]^{3-}$ structure, to provide that $\alpha-[Mo_{0(12-x)}V_xPO_{40}]^{(3+x)-}$ isomer. For dissymmetric isomers, the degeneracies of their enantiomorphs are added together.

Received November 1, 1999
[199390]